

LA-UR-10-07086

*Approved for public release:
distribution is unlimited.*

*Title: Longitudinal Losses Due to Breathing Mode
Excitation in Radiofrequency Linear Accelerators*

Author(s): Paul J. Channell

Intended for:



Los Alamos National Laboratory, an affirmative action/equal opportunity employer, is operated by the Los Alamos National Security, LLC for the National Nuclear Security Administration for the U.S. Department of Energy under contract DE-AC52-06NA25396. By acceptance of this article, the publisher recognizes that the U.S. Government retains a nonexclusive, royalty-free license to publish or reproduce the published form of this contribution, or to allow others to do so, for U.S. Government purposes. Los Alamos National Laboratory requests that the publisher identify this article as work performed under the auspices of the U.S. Department of Energy. Los Alamos National Laboratory strongly supports academic freedom and a researcher's right to publish; as an institution, however, the Laboratory does not endorse the viewpoint of a publication or guarantee its technical correctness.

Form 836 (7/06)

Longitudinal Losses Due to Breathing Mode Excitation in Radiofrequency Linear Accelerators

Paul J. Channell*
MS H808
Los Alamos National Laboratory
Los Alamos, NM 87545

Abstract

Transverse breathing mode oscillations in a particle beam can couple energy into longitudinal oscillations in a bunch of finite length and cause significant losses. We develop a model that illustrates this effect and explore the dependence on mismatch size, space-charge tune depression, longitudinal focusing strength, bunch length, and RF bucket length.

*pchannell@lanl.gov

1 Introduction

In high average power radiofrequency (RF) linacs the problem of losses can be acute, as they tend to activate the structure. Depending on the average beam power, loss fractions less than one part in a million may be required. Previously people, [2], [3], [4], have examined the role of transverse breathing mode oscillations on transverse losses and concluded that they could drive particles out to several times the original beam size. Of course, in modern superconducting RF accelerators with strong focusing, the wall radius can be many times the beam size so these oscillations may not lead to unacceptable losses.

However, these breathing mode oscillations can also couple to the longitudinal oscillations in a finite length bunch and cause particles to move outside the RF bucket. In that case, particles will eventually have an energy so far away from the design energy that they will be lost transversely. Note that typically the length of the RF bucket is only a few times the length of the particle bunch (for protons or ions) so a detailed investigation is required.

In this paper we examine the effect of transverse breathing mode oscillations on the longitudinal oscillations of particles and show that in some circumstances the resulting losses can be very significant.

2 Model

In this article we will investigate beam loss in the longitudinal direction caused by a type of deterministic diffusion in a finite length mismatched beam. A mismatch causes envelope oscillations that are approximately described by the equation

$$\frac{d^2 X}{dt^2} + X - \frac{\eta^2}{X^3} - \frac{I}{X} = 0, \tag{1}$$

where X is the envelope amplitude, η is the tune depression parameter, and $I \equiv 1 - \eta^2$. Note that if $X = 1$ and $\frac{dX}{dt} = 0$ then the breathing mode has zero amplitude, i.e. the envelope doesn't oscillate.

The transverse motion of a single particle in the resulting oscillating hard-edge beam has been described by Gluckstern, Wangler and others, [2] [3], for one transverse degree of freedom and is given by the equation

$$0 = \frac{d^2x}{dt^2} + x - \begin{cases} \frac{Ix}{X^2} & \text{if } x < X \\ \frac{I}{x} & \text{if } x > X \end{cases} \quad (2)$$

The discontinuity in derivative at $x = X$ is awkward, so we replace this equation by

$$0 = \frac{d^2x}{dt^2} + x - \frac{Ix}{x^2 + X^2}, \quad (3)$$

a continuous version which has the same behavior as the original equation. The transverse phase space diagram for this equation is the standard ‘peanut’ shape shown in figure 1.

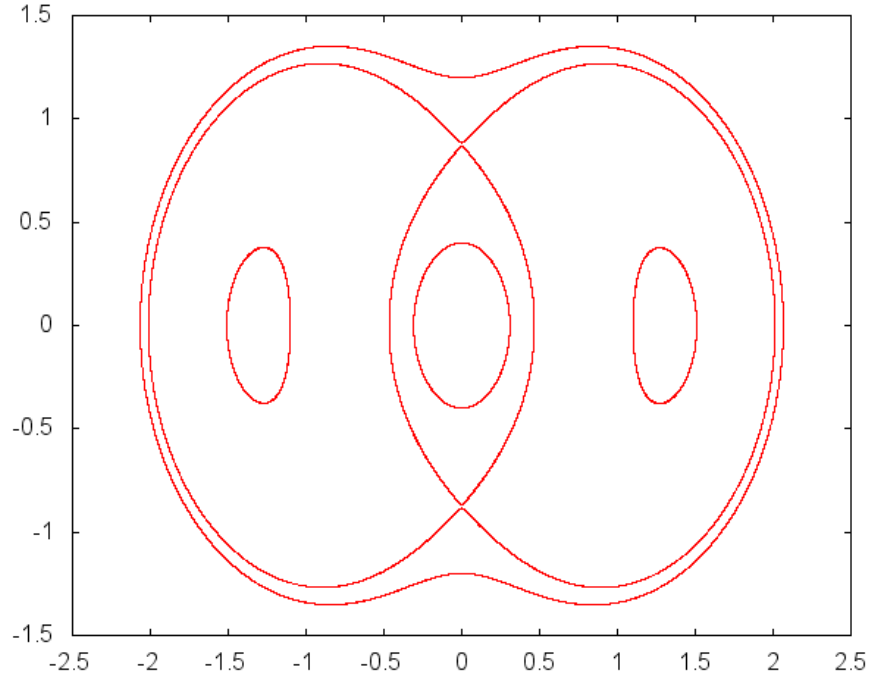


Figure 1: Five transverse trajectories of the uncoupled system illustrating the usual ‘peanut’ phase space.

We now want to incorporate the longitudinal motion of particles in a finite length bunch. Without coupling we take the longitudinal motion to be described by

$$0 = \frac{d^2z}{dt^2} + \frac{\omega_z^2 b}{2\pi} \sin\left(\frac{2\pi z}{b}\right), \quad (4)$$

i.e. a simple pendulum with small amplitude angular oscillation frequency ω_z , and an effective length of b , the ‘bucket’ length. In a real RF linac the bucket shape is more complicated but this model should capture the effect of nonlinear longitudinal oscillations and a finite length region of longitudinal stability. Note that these equations for the particle motion can be derived from the Hamiltonian

$$H = \frac{p_x^2}{2} + \frac{x^2}{2} + \frac{p_z^2}{2} - \frac{\omega_z^2 b^2}{4\pi^2} \cos\left(\frac{2\pi z}{b}\right) - \frac{I}{2} \ln(x^2 + X^2). \quad (5)$$

In order to have a simple model of the coupling of longitudinal and transverse motion, we let

$$I = I_0 e^{-\frac{z^2}{L^2}}, \quad (6)$$

where L is a bunch length. Note that in a real finite length bunch the envelope oscillation would not retain the simple form we have assumed here; thus our model is overly simplified but should be indicative of the type of physics that can occur. The Hamiltonian now becomes

$$H = \frac{p_x^2}{2} + \frac{x^2}{2} + \frac{p_z^2}{2} - \frac{\omega_z^2 b^2}{4\pi^2} \cos\left(\frac{2\pi z}{b}\right) - \frac{I_0 e^{-\frac{z^2}{L^2}}}{2} \ln(x^2 + X^2). \quad (7)$$

The equations of motion that result from this coupled Hamiltonian are

$$\frac{dx}{dt} = p_x, \quad (8)$$

$$\frac{dp_x}{dt} = -x + \frac{I_0 e^{-\frac{z^2}{L^2}} x}{x^2 + X^2}, \quad (9)$$

$$\frac{dz}{dt} = p_z, \quad (10)$$

and

$$\frac{dp_z}{dt} = -\frac{\omega_z^2 b}{2\pi} \sin\left(\frac{2\pi z}{b}\right) + \frac{I_0 z}{L^2} \ln(x^2 + X^2) e^{-\frac{z^2}{L^2}}. \quad (11)$$

Note that as $L \rightarrow \infty$ these equations reduce to the uncoupled equations.

The driving mechanism for the particle instability and loss we observe in this model is the transverse envelope oscillation and its modulation due to the longitudinal change in space charge strength along the bunch. Another term could come from coupling transverse space charge oscillations to longitudinal space charge oscillations which would also drive particles longitudinally. A simple model of this effect does not yet exist, so we won't include this term in this paper.

2.1 Model Parameters

The model we use has a number of parameters that can be varied. The transverse angular betatron frequency is $\omega_\beta = 1$ and does not vary. The longitudinal angular oscillation frequency, ω_z , is a measure of the strength of the longitudinal focusing. The bunch length is measured by L ; the actual bunch length (95% included) is about $4L$ if the bunch is Gaussian. The bucket length, b , depends on the accelerating phase and may be half of the RF wavelength (no acceleration), but is typically less than a quarter of the RF wavelength. Note that the bucket ranges from $-b/2$ to $b/2$ in z . The tune depression parameter is η and ranges from 1 (no space charge) down to small values for high space charge. Finally there is the initial value of the envelope oscillation, X_0 , which is 1 for no oscillation. (We always take the initial $\frac{dX}{dt} = 0$.) We take various values of the initial X_0 ranging from 0.9 down to 0.45; the envelope oscillation is nonlinear but is such that the maximum X is approximately $2 - X_0$; the oscillation is very roughly symmetrical about $X = 1$. The period of the envelope oscillation depends on the amplitude of the oscillation, but is near 4 for the range we consider.

2.2 Reason for instability

To understand the reason the transverse envelope oscillation can drive longitudinal oscillations consider figure 2 where we plot in three dimensions the trajectories of two points starting at the same transverse phase space location but with different longitudinal oscillation amplitudes. What is shown is a stroboscopic plot taken at exactly period intervals of the envelope oscillation, a cross section in mathematical terminology. The picture shown has no longitudinal-transverse coupling. Each trajectory is a product of an ellipse in the longitudinal phase space (we show only one longitudinal phase space variable) with an unstable trajectory of the 'peanut' in the transverse phase

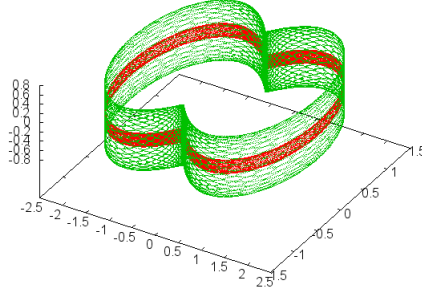


Figure 2: Two trajectories (one red, one green) starting at the same transverse location but with different longitudinal energies. These lie on ‘whiskers’ of the unstable whiskered tori.

space. Note that the transverse unstable ellipse (point when projected only onto the transverse plane) at the cusp of the shown trajectories is actually an ellipse crossed into a circle since time is periodic and doesn’t appear in the stroboscopic slice; thus it is a two-dimensional torus. The trajectories shown (which are three dimensional when time is included) lie on what Arnold, [1], calls ‘whiskers’ of the whiskered tori which are the two dimensional unstable points crossed ellipses crossed periodic time. Note that in this case the whiskers don’t look much like real whiskers so the name is misleading. In the pictured uncoupled case these whiskers don’t intersect and no instability can occur. However, when coupling is added to the model, the whiskers from two different longitudinal oscillation amplitudes do generically intersect and connect initial conditions with small longitudinal oscillation amplitudes to trajectories with large longitudinal oscillation amplitudes, leading to instability and particle loss. Thus, the energy of the transverse envelope oscillation can be pumped into the longitudinal oscillations of particles leading to longitudinal losses. Of course it is important to determine the magnitudes of the losses for various parameters and determine the most important variables to be controlled. Determining the losses analytically would be very difficult so we will use simulation of the above model to get an indication of loss rates.

3 Simulation

All simulations were done using a fourth order symplectic integrator, [5]. For each set of parameters and envelope initial condition the envelope period was first determined using a very tiny time step, i.e. to double precision accuracy. Particle trajectories were then printed out at multiples of this envelope period so that stroboscopic pictures could be made. The envelope oscillation was computed numerically at each time step along with the trajectories of the particles.

In all the simulations reported here the particles were initialized with very small longitudinal momentum. In longitudinal position the particles were chosen to be uniformly random in the interval $[-0.67L, 0.67L]$ where L is the bunch length parameter; note that we are not using the same distribution for the test (simulation) particles that we assume for the space-charge model. In the transverse direction the initial conditions were chosen to be uniformly random in both x and p_x in the interval $[-0.335, 0.335]$ where the unstable transverse point is at about $[0, 0.87]$, (it varies depending on parameters).

Integrations were carried out with 2000 steps per envelope period and the integration was carried out for 100 envelope periods. The number of particles in the simulations was 4000. Particles were counted as lost when the absolute magnitude of their longitudinal position exceeded $b/2$.

Simulations were done varying X_0 over the values (0.45, 0.6, 0.75, 0.9), η over the values (0.35, 0.5, 0.65, 0.8), ω_z^2 over the values (0.01, 0.11, 0.21, 0.31), the bucket length, b , over the values (10, 15, 20, 25), and the bunch length parameter, L , over the values (2, 3, 4, 5, 6). A total of 704 simulations were done, namely those that had bunch lengths ($4L$) less than the bucket length (b). We report the results of these 704 simulations.

4 Results

Of the 704 cases, 158 led to particle losses ranging from 1 particle (out of 4000) to 100% of the particles. More than 10% losses occurred in 101 cases, and greater than 1% losses occurred in a further 27 cases. A phase space plot of a case with only 1% particles lost is shown in figure 3.

The correlation coefficients of the particle losses with the variables are shown in table 1. As can be seen, all the variables affect the particle losses, though the dependence on L is quite weak. The directions of the correlations

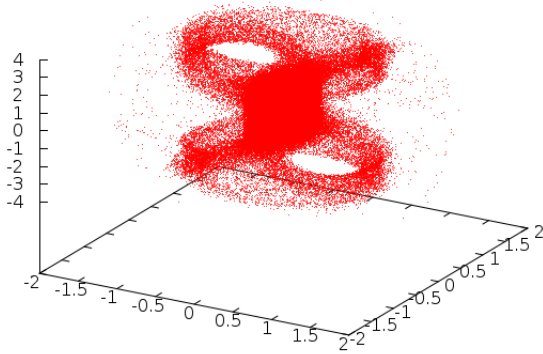


Figure 3: Stroboscopic phase space plot of a case with only 1% of the particles lost. The three dimensional projection (x, p_x, z) of 4000 particles at 100 envelope periods are shown; though not all points are shown as the lost particles move out to larger longitudinal positions.

are what one would expect, i.e. one has lower losses with a) smaller mismatch, b) less space charge (less current), c) stronger longitudinal focusing, d) longer bucket lengths, and e) shorter bunches.

In more detail, note that all values of mismatch, even small ones ($X_0 = 0.9$), can lead to particle losses. Any particle loss in our simulations, a part in 4000, is greater than most high power linacs can allow. Also, particle losses can occur for all values of the space charge, including very low space charge, $\eta = 0.9$, though they tend to be worse for higher space charge. The longitudinal focusing strength in our simulations ranged from moderate ($\omega_z^2 = 0.01$) to very strong, ($\omega_z^2 = 0.31$ which is nearly 1/3 the transverse focusing strength) and particle losses occurred for all cases. The strongest dependence on the model parameters was on the longitudinal focusing strength. No one parameter can guarantee no losses, though there are only a few cases with loss for the largest longitudinal focusing.

In table 2 we give the parameters and fractional losses for the thirty cases with largest losses. Note that all values of mismatch, space charge, bucket length, and bunch length occur. However, only the smallest longitudinal

Variable	Correlation coefficient
X_0	-0.2885519
η	-0.1515029
ω_z^2	-0.4810484
b	-0.1672322
L	-0.0471679

Table 1: Correlation coefficients of losses with model variables.

focusing frequency occurs for these high loss cases. Unfortunately, this lowest longitudinal focusing strength is also the case most typical of RF linacs. Note that by assuming small mismatch and small space charge it is possible for cases with this lowest longitudinal focusing strength to have no losses.

If we look at the projections of the fractional losses on the various two dimensional subspaces of the variables we get the three dimensional figures shown. In figures 5b, 7a, 8a, and 8b one notes the very weak dependence on the bunch length found in the correlation coefficients. In figures 4b, 6a, 7b, and 8a one notes the strong dependence on longitudinal focusing strength also found in the correlation coefficients. The moderate dependence of losses on mismatch can be seen in figures 4a, 4b, 5a, and 5b. The weak dependence of losses on space charge can be seen in figures 4a, 6a, 6b, and 7a. The dependence of losses on bucket length can be seen in figures 5a, 6b, 7b, and 8b; it seems to be significant only for the shortest buckets.

4.1 An extended model

At the suggestion of Yuri Batygin we have extended the previous model to include RF nonlinearity; in particular we studied the model Hamiltonian

$$H = \frac{p_x^2}{2} + \frac{x^2}{2} + \frac{p_z^2}{2} - \frac{\omega_z^2 b^2}{4\pi^2} \cos\left(\frac{2\pi z}{b}\right) - \frac{I}{2} \ln(x^2 + X^2) + \frac{b\alpha x^2}{2\pi} \sin\left(\frac{2\pi z}{b}\right), \quad (12)$$

where α controls the magnitude of the RF nonlinearity. Setting the bunch length parameter, $L = 3.0$, we performed 768 simulations with

$$\alpha = 0.003, 0.006, 0.009, 0.012;$$

the largest value gives a nonlinear betatron frequency shift at the ends of the bunch of about $\pm 9\%$. Note that the additional term is antisymmetric about

X_0	η	ω_2^2	b	L	Loss
0.45	0.35	0.01	10.	2.	1.
0.45	0.35	0.01	15.	3.	1.
0.45	0.50	0.01	10.	2.	1.
0.45	0.50	0.01	15.	3.	1.
0.45	0.65	0.01	10.	2.	1.
0.45	0.80	0.01	10.	2.	1.
0.45	0.35	0.01	15.	2.	0.9995
0.60	0.50	0.01	10.	2.	0.99875
0.45	0.50	0.01	15.	2.	0.9965
0.45	0.65	0.01	15.	3.	0.99625
0.60	0.65	0.01	10.	2.	0.991
0.45	0.35	0.01	20.	3.	0.985
0.45	0.65	0.01	15.	2.	0.98275
0.45	0.50	0.01	20.	4.	0.979
0.45	0.50	0.01	20.	3.	0.96125
0.45	0.35	0.01	20.	2.	0.95925
0.45	0.65	0.01	20.	4.	0.93275
0.60	0.50	0.01	15.	2.	0.9215
0.45	0.50	0.01	25.	4.	0.914
0.45	0.35	0.01	25.	3.	0.90075
0.60	0.35	0.01	10.	2.	0.8845
0.60	0.80	0.01	10.	2.	0.882
0.45	0.65	0.01	20.	3.	0.881
0.45	0.35	0.01	25.	2.	0.859
0.60	0.35	0.01	15.	2.	0.841
0.45	0.35	0.01	20.	4.	0.8195
0.45	0.35	0.01	25.	4.	0.813
0.45	0.35	0.01	25.	6.	0.80075
0.45	0.65	0.01	25.	6.	0.8005
0.45	0.50	0.01	25.	5.	0.788

Table 2: Thirty cases with largest fractional losses.

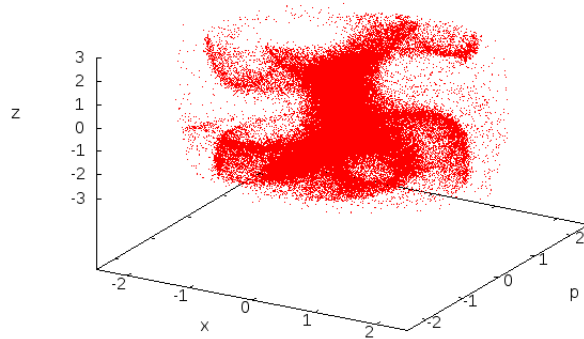


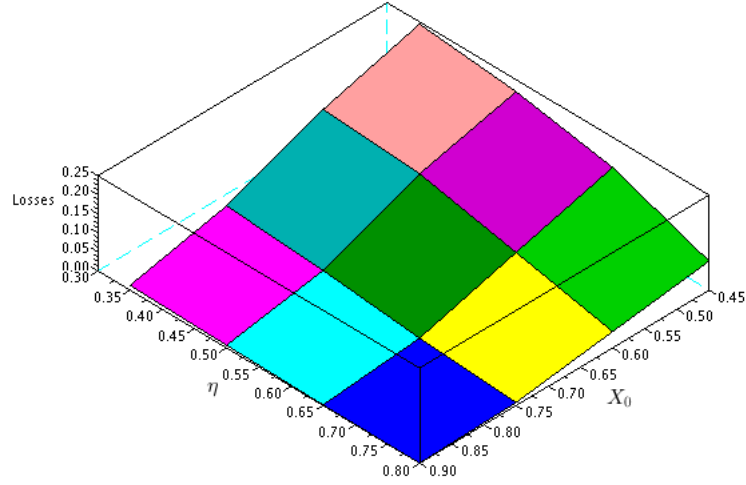
Figure 4: Stroboscopic phase space plot of a case with only 1% of the particles lost. The three dimensional projection (x, p_x, z) of 4000 particles at 100 envelope periods are shown; though not all points are shown as the lost particles move out to larger longitudinal positions. Note the asymmetry in z evident in the plot.

the bunch center and this antisymmetry can be seen in the phase space plot in figure 4.

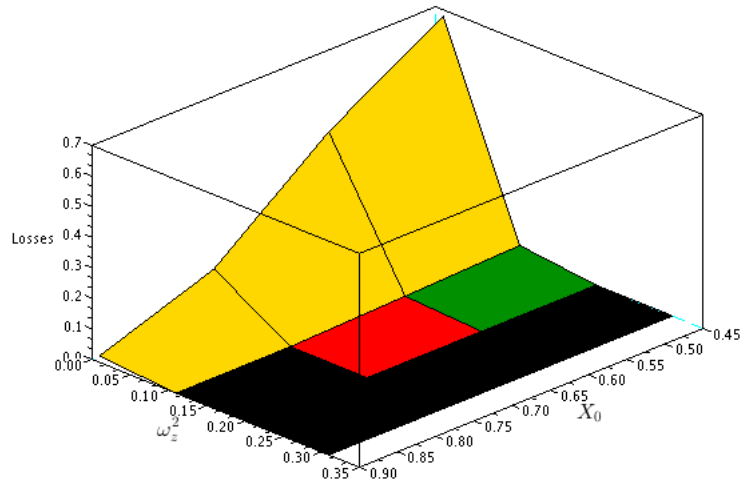
The results of these simulations with the extended model are essentially the same as those from the previous model. In particular the correlation coefficient of the losses with the α parameter is 0.0035, i.e. is consistent with 0. The projection graphs for this case are essentially the same as figures 5 – 9 (when the variables coincide) so we will not show them again.

5 Conclusions

No single parameter guarantees no losses in our simulations, though smaller mismatch and larger longitudinal focusing have the strongest effect in reducing losses. Less space charge and longer bucket lengths have significant, though smaller effects on losses and bunch length is relatively unimportant. The nonlinearity of the RF seems to have very little effect on the losses.



(a)



(b)

Figure 5: Projected losses as functions of a) X_0 and η , b) X_0 and ω_z^2 . Smaller losses occur for smaller mismatch (X_0 closer to 1), smaller space charge (η closer to 1), and larger longitudinal focusing, larger ω_z^2 , with this dependence rather strong.

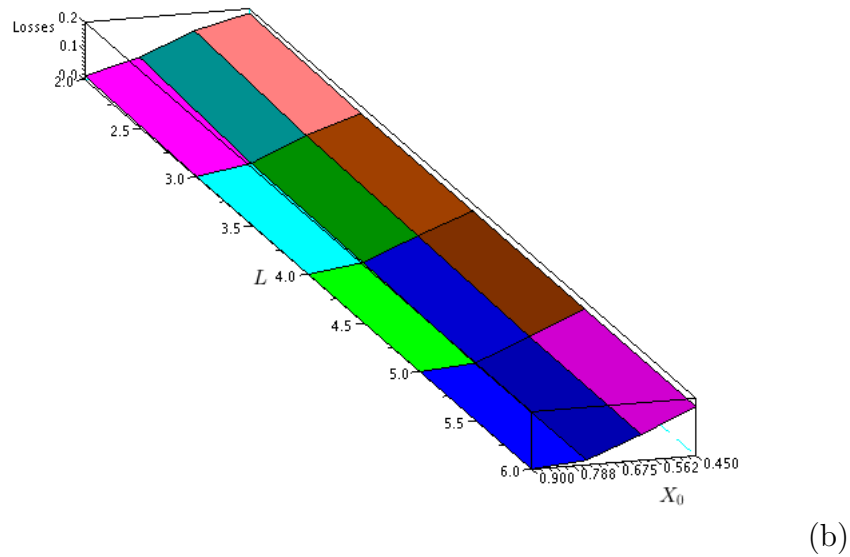
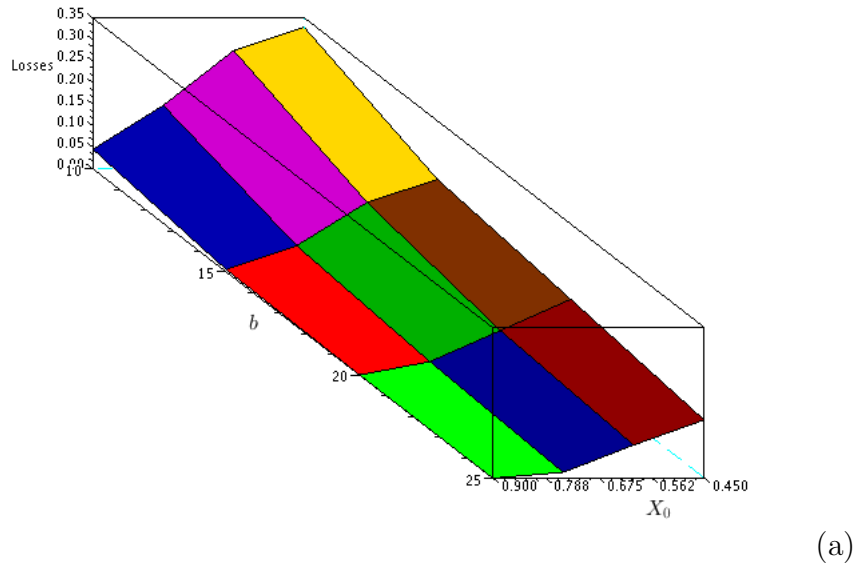
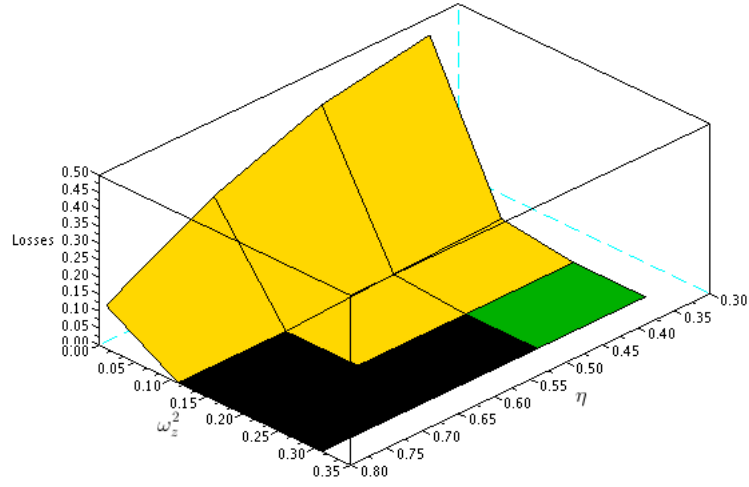
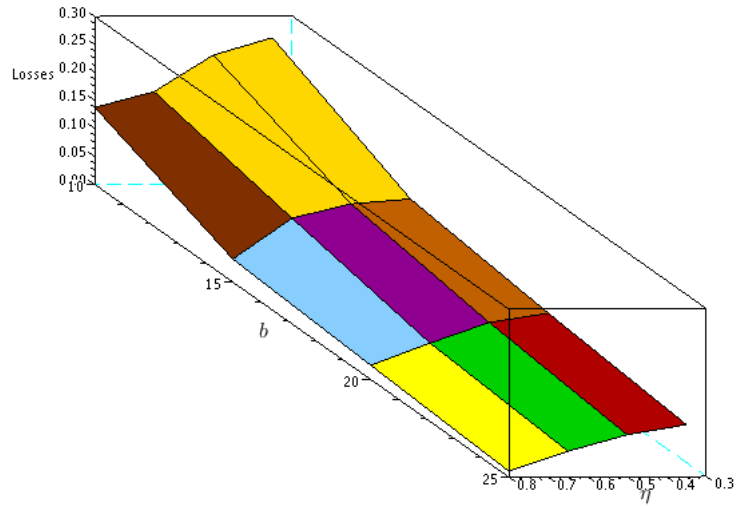


Figure 6: Projected losses as functions of a) X_0 and b , and b) X_0 and L . Smaller losses occur for larger bucket lengths, b , and shorter bunches, L , though the latter dependence is quite weak. The dependence on bucket length is strongest for short buckets.

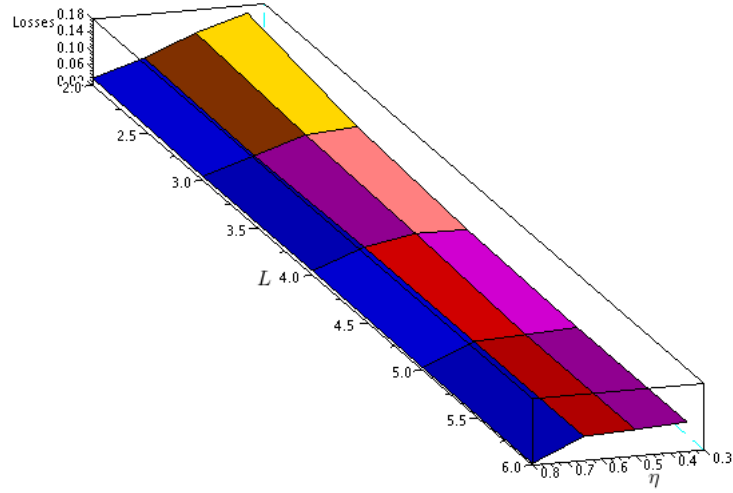


(a)

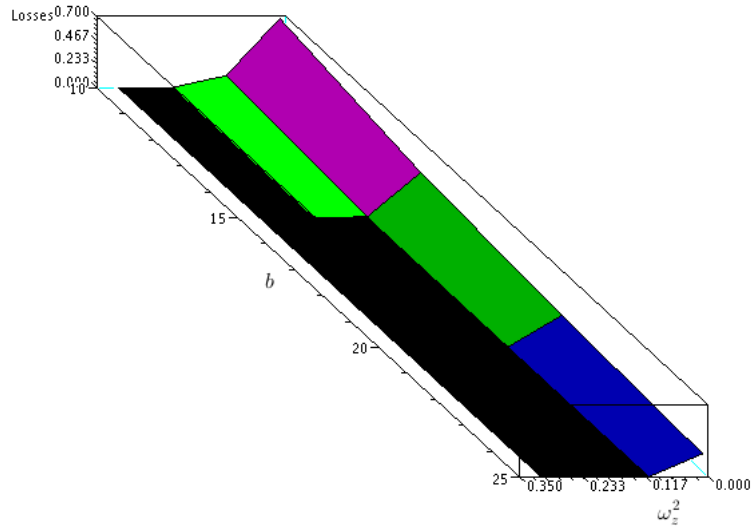


(b)

Figure 7: Projected losses as functions of a) η and ω_z^2 , b) η and b . Losses are smaller for less space charge, (η larger), stronger longitudinal focusing, and larger bucket lengths.

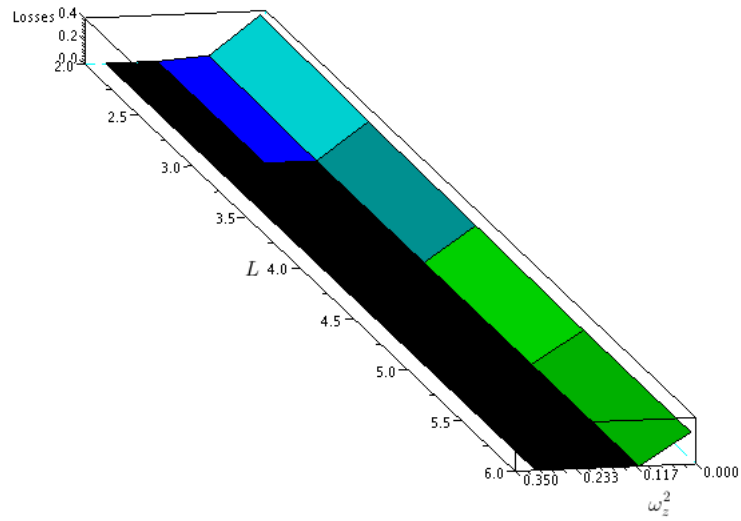


(a)

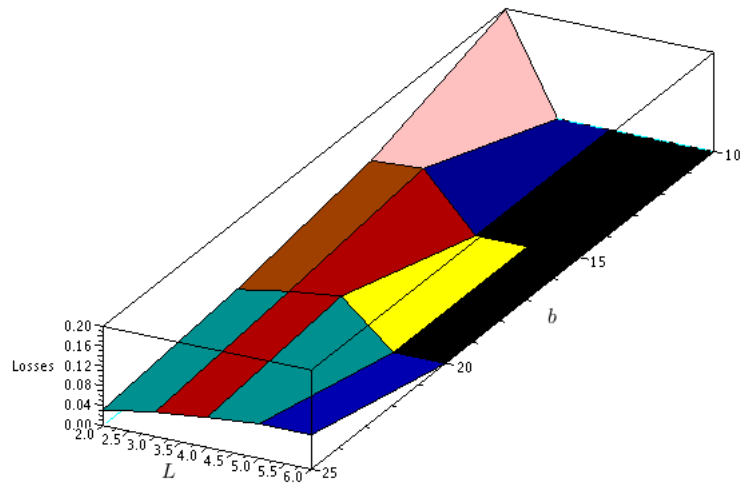


(b)

Figure 8: Projected losses as functions of a) η and L , and b) ω_z^2 and b . The losses depend weakly on bunch length and on bucket length and more strongly on longitudinal focusing strength.



(a)



(b)

Figure 9: Projected losses as functions of a) ω_z^2 and L , b) b and L . the losses depend most strongly on ω_z^2 .

Acknowledgments Conversations with and suggestions from Yuri Batygin and Tom Wangler are greatly appreciated.

References

- [1] Arnold, Vladimir I. ‘Instability of dynamical systems with several degrees of freedom’. Soviet Mathematics Dokl. 5: (1964) pp. 581-585.
- [2] R. L. Gluckstern, *Phys. Rev. Lett.***73** (1994) p. 1247.
- [3] T. P. Wangler, R. W. Garnett, E. R. Gray, R. D. Ryne, and T. S. Wang, Proc. 18th Int. Linear Accel. Conf. August 26-30, 1996, Geneva, CERN 96-07, p. 372.
- [4] T. P. Wangler, K.R. Crandall, R. D. Ryne, and T. S. Wang, *Phys. Rev. Special Topics, Accelerators and Beams*, **1**, 1998, 084201.
- [5] Yoshida, H., ‘Construction of higher order symplectic integrators’, *Phys. Lett. A***150** (1990) pp. 262-268.